Electronic Supplementary Information

Selective furfural hydrogenolysis towards 2-methylfuran by controlled poisoning of Cu-Co catalysts with chlorine

Alberto Barranca[a], Iker Agirrezabal-Tellería[a], Marcos Rellán-Piñeiro[b], Manuel A. Ortuño[b], I. Gandarias[a]*

[a] Department of Chemical and Environmental Engineering. Faculty of Engineering Bilbao. University of the Basque Country UPV/EHU. Plaza Ingeniero Torres Quevedo 1. 48013 Bilbao (Spain).
[b] Centro Singular de Investigación en Química Biolóxica e Materiais Moleculares (CIQUS), Universidade de Santiago de Compostela, 15782 Santiago de Compostela, Spain.
* Correspondence: inaki.gandarias@ehu.eus; Tel.: +34 94 6017373

Contents **Page**

1 Figures

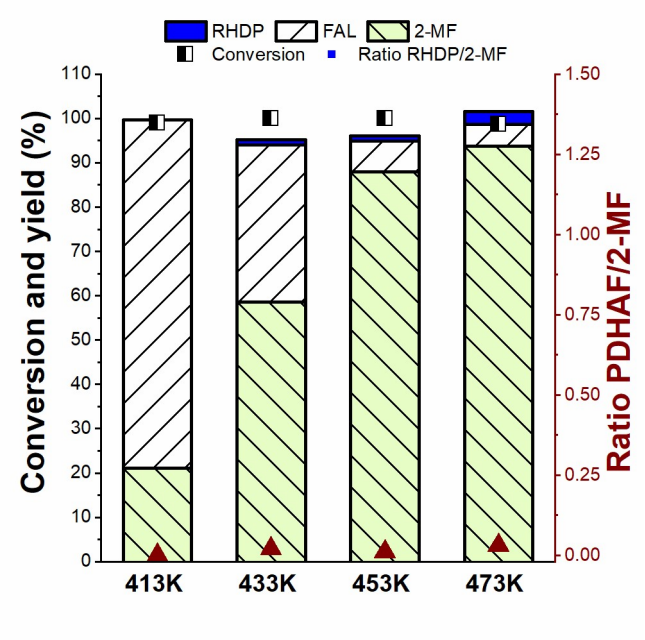

Figure S1. Furfural conversion, yield of the different products and RHDP/2-MF ratio for the Cu^{N}-Co^{Cl}/γ-Al_2O_3 catalyst at different reaction temperatures. 3 MPa hydrogen, 0.250 g_{cat} g_{FUR}^{-1}, 3.5 h.

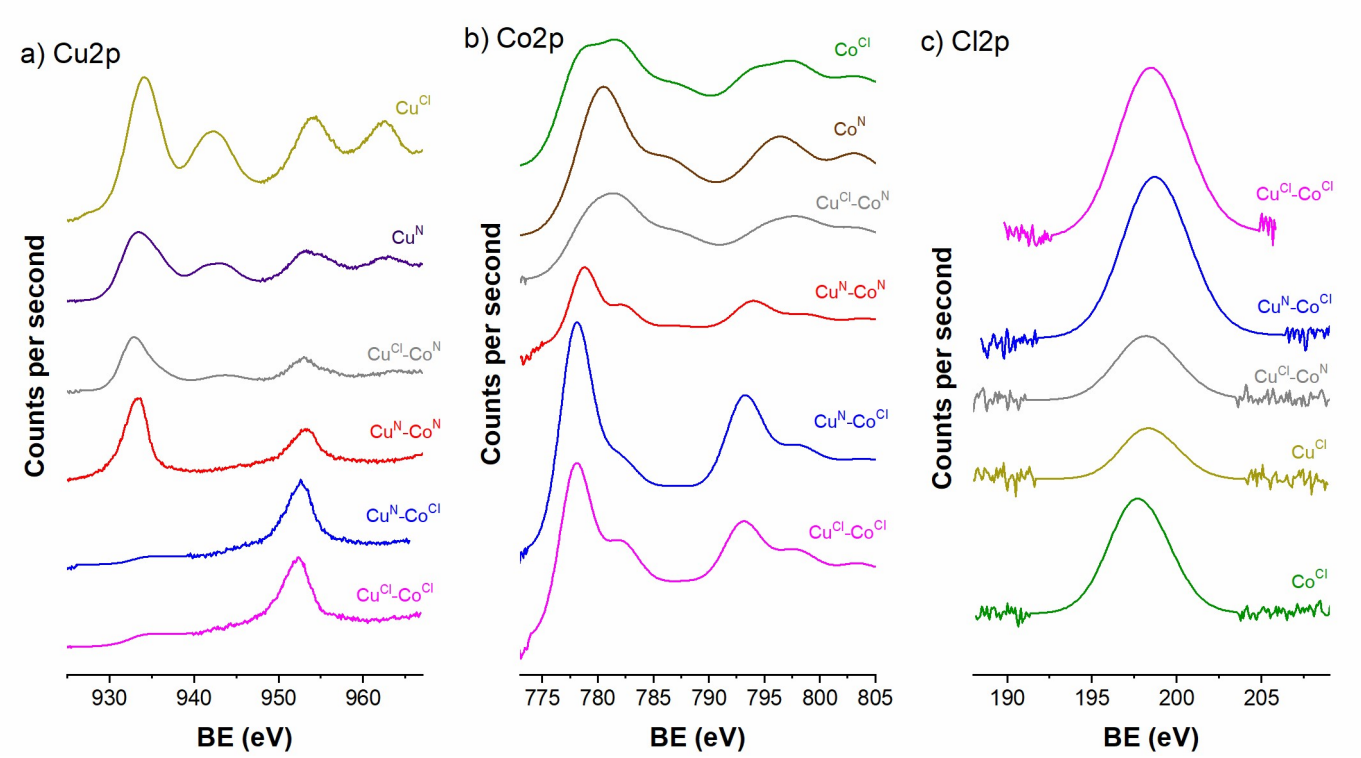

Figure S2. Cu 2p core-level (a), Co 2p core-level (b) and Cl 2p core-level (c), spectra of reduced Cu^{x}-Co^{y}/γ-Al_2O_3 series.

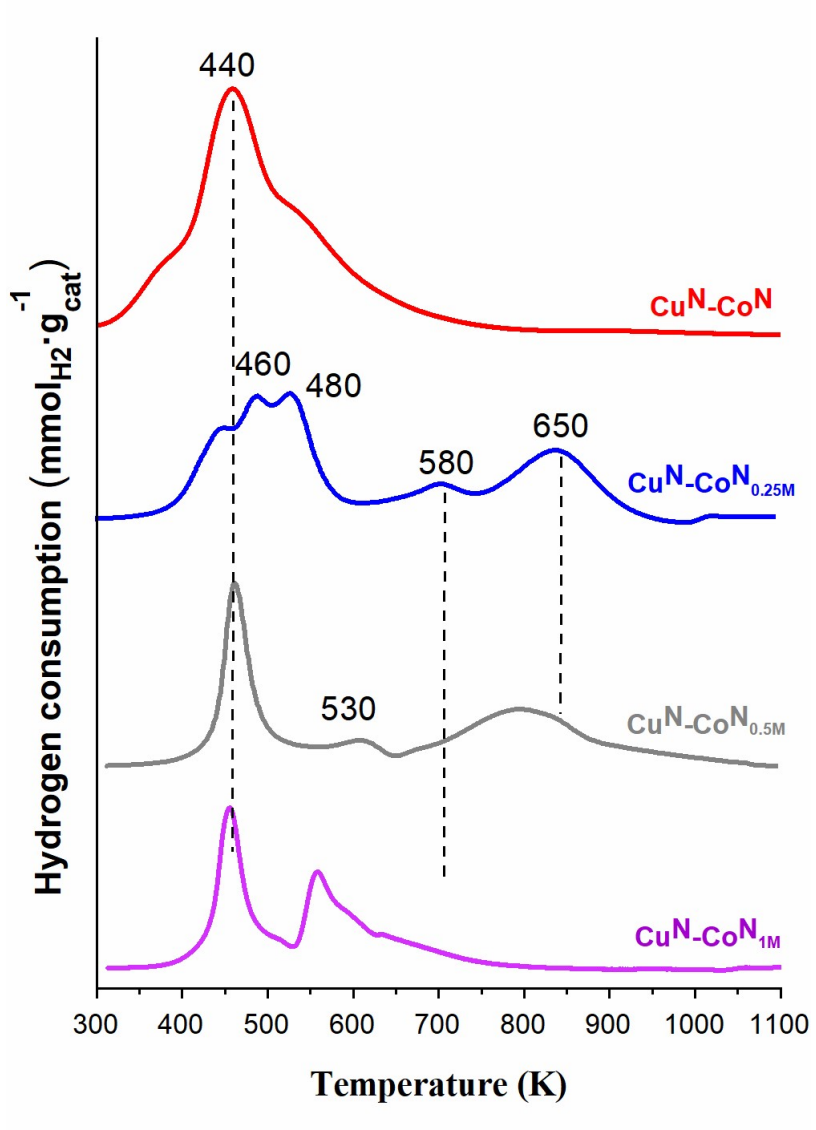

Figure S3. H_2-TPR for bimetallic Cu^N-$Co^N_{[x]}$ catalytic series.

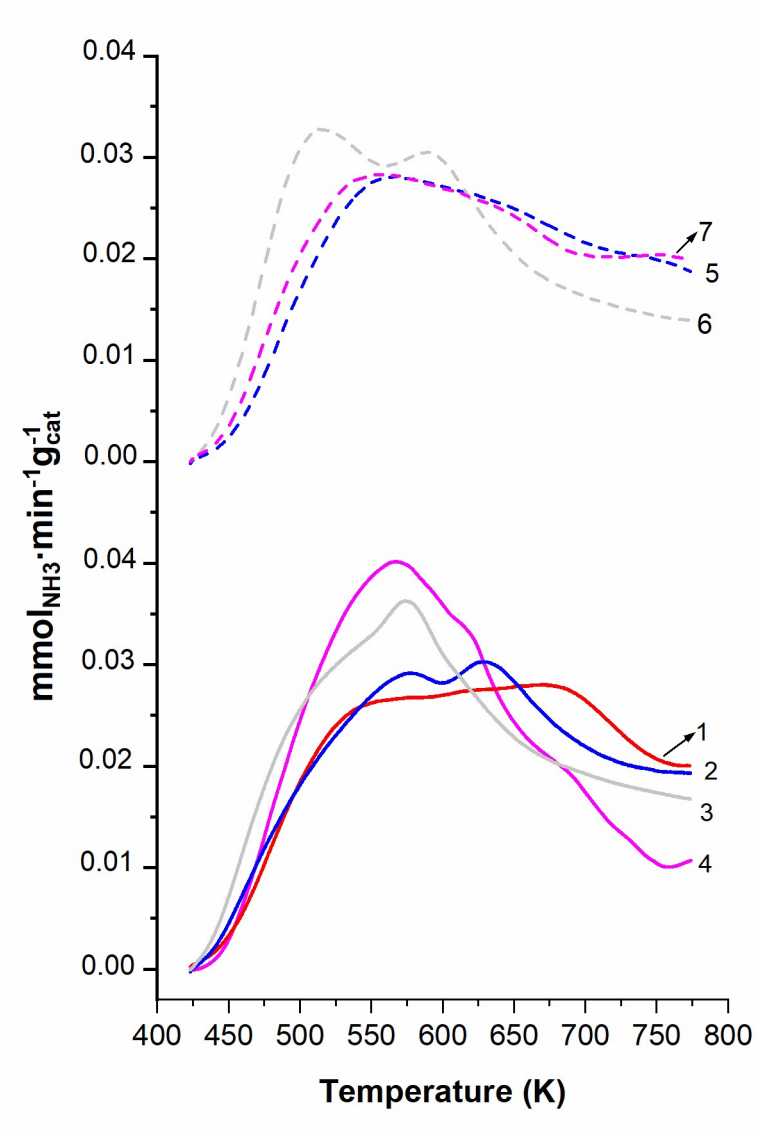

Figure S4. TPD-NH_3 profiles for: 1) Cu^{N}-Co^{N}; 2) Cu^{N}-$Co^{N}_{[0.25M]}$; 3) Cu^{N}-$Co^{N}_{[0.5M]}$; 4) Cu^{N}-$Co^{N}_{[1M]}$; 5) Cu^{Cl}-$Co^{Cl}_{[0.25M]}$; 6) Cu^{Cl}-$Co^{Cl}_{[0.5M]}$; 7) Cu^{Cl}-$Co^{Cl}_{[1M]}$

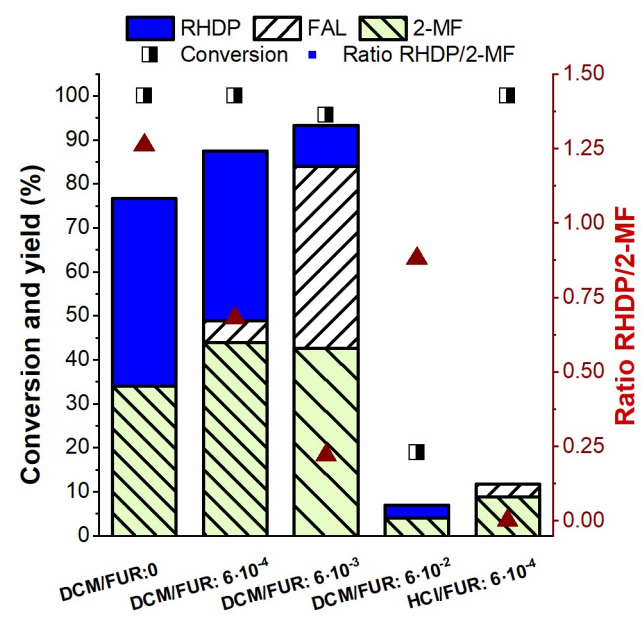

Figure S5. Furfural conversion, yield of the different products and RHDP/2-MF ratio for the Cu^{N}-Co^{N} catalyst at different dichloromethane (DCM):furfural and HCl:furfural ratios in the reaction medium. 3 MPa hydrogen, 0.250 g_{cat} g_{FUR}^{-1}, 3.5 h.

2 Tables

Table S1. Operating conditions and results obtained in the activity tests of the Cu^{x}-Co^{y} series. All experiments were carried out at a P_{H2} = 30 bar and 3.5 h reaction time.

Entry	Catalyst /γ-Al_2O_3	$g_{cat}\ g_{FUR}^{-1}$	T (K)	Conv. (%)	Yield (%)				Ratio RHDP/2-MF	Prod. ($mol_{2MF}\ kg_{cat}^{-1}\ h^{-1}$)	CB (%)
					2-MF	FAL	THFA	PDOs			
1	Cu^{Cl}	0.125	453	10.1	2.20	3.20	0.00	0.00	0.00	0.50	95.3
2	Co^{N}	0.125	453	100	31.1	33.2	10.7	8.80	0.62	7.10	82.0
3	Cu^{N}	0.125	453	100	9.10	79.0	0.00	0.90	0.10	2.08	88.1
4	Co^{Cl}	0.125	453	72.0	22.1	46.5	0.00	0.00	0.00	5.05	98.0
5	Cu^{Cl}-Co^{Cl}	0.125	453	100	51.5	34.3	0.00	0.00	0.00	11.8	85.8
6	Cu^{Cl}-Co^{N}	0.125	453	100	56.5	31.5	0.00	2.30	0.04	12.9	90.3
7	Cu^{N}-Co^{Cl}	0.125	453	100	61.5	36.6	0.00	0.00	0.00	14.1	98.1
8	Cu^{N}-Co^{N}	0.125	453	100	34.0	0.00	17.6	25.2	1.26	7.77	76.8
9	Cu^{N}-Co^{Cl}	0.250	413	98.7	21.3	78.6	0.00	0.00	0.00	2.30	98.7
10	Cu^{N}-Co^{Cl}	0.250	433	100	58.6	30.7	0.00	1.20	0.02	7.10	95.1
11	Cu^{N}-Co^{Cl}	0.250	453	100	87.9	7.10	0.00	1.10	0.01	10.3	96.1
12	Cu^{N}-Co^{Cl}	0.250	473	100	93.8	4.90	0.70	2.20	0.03	11.5	100

Table S2. Operating conditions and results obtained in the activity tests of the Cu^{N}-$Co^{N}_{[X]}$ and Cu^{Cl}-$Co^{Cl}_{[X]}$ series. Operating conditions: P_{H2} =30 bar H_2; T = 453 K; $g_{cat}\ g_{FUR}^{-1}$ = 0.125

Entry	Catalyst /γ-Al_2O_3	Conv. (%)	Yield (%)				Ratio RHDP/2-MF	Product. ($mol_{2MF}\ kg_{cat}^{-1} h^{-1}$)	CB (%)
			2-MF	FAL	THFA	PDOs			
1	Cu^{N}-Co^{N}	100	34.0	0.00	17.6	25.2	1.26	7.77	76.8
2	Cu^{N}-$Co^{N}_{[0.25M]}$	99.9	59.9	24.3	0.00	2.77	0.05	13.7	87.4
3	Cu^{N}^$Co^{N}_{[0.5M]}$	100	77.2	22.0	0.00	3.89	0.05	17.7	103
4	Cu^{N}^$Co^{N}_{[1M]}$	100	53.2	44.6	0.00	4.03	0.08	12.2	105
5	Cu^{Cl}-Co^{Cl}	100	51.5	34.3	0.00	0.00	0.00	11.8	85.8
6	Cu^{Cl}^$Co^{Cl}_{[0.25M]}$	97.8	51.7	48.1	0.00	0.00	0.00	11.8	101
7	Cu^{Cl}^$Co^{Cl}_{[0.5M]}$	92.6	21.2	70.7	0.00	0.00	0.00	4.83	99.3
8	Cu^{Cl}^$Co^{Cl}_{[1M]}$	41.7	8.44	47.0	1.24	0.00	0.14	1.93	114

Table S3. Binding energies for the surface species detected in the reduced Cu^{N}-$Co^{N}_{[x]}$ and Cu^{Cl}-$Co^{Cl}_{[x]}$ catalytic series.

XPS Results										
Entry	**Catalyst /Al_2O_3**	**Be Cu^0 $2p_{3/2}$ (eV)**	**Be Cu^{2+} $2p_{3/2}$ (eV)**	**Be Co^0 $2p_{3/2}$ (eV)**	**Be Co^{x+} $2p_{3/2}$ (eV)**	**Be Cl^- $2p_{3/2}$ (eV)**	**% at. Cl**	**Cu^0/Cu^{2+}**	**Co^0/Co^{x+}**	**Cl/(Co+Cu)**
1	Cu^{N}-Co^{N} $_{[0.25M]}$	932.9	-	778.6	782.7	198.5	1.2	TR	1.2	0.38
2	Cu^{N}-Co^{N} $_{[0.5M]}$	933.2	-	778.5	782.4	197.8	2.4	TR	1.6	0.40
3	Cu^{N}-Co^{N} $_{[1M]}$	933.2	-	778.4	782.5	197.6	3.4	TR	1.2	0.67
4	Cu^{Cl}-Co^{Cl} $_{[0.25M]}$	932.1	-	777.6	781.6	198.2	3.5	TR	1.3	0.43
5	Cu^{Cl}-Co^{Cl} $_{[0.5M].}$	932.8	-	778.1	782.4	197.6	3.8	TR	1.1	0.46
6	Cu^{Cl}-Co^{Cl} $_{[1M]}$	932.6	-	777.9	782.2	198.0	5.1	TR	0.5	0.62

Table S4. Binding energies and percentage of atomic content for the Cl species detected in the spent (after activity test) Cu^{N}-Co^{N} catalyst with different DCM:FUR and HCl:FUR ratios; and for Cu^{N}-$Co^{N}_{[0.5M]}$ after conventional activity test.

XPS Results					
Entry	**Catalyst /Al_2O_3**	**DCM:FUR**	**HCl:FUR**	**Be Cl^- $2p_{3/2}$ (eV)**	**% at. Cl**
1	Cu^{N}-Co^{N}	$6{\cdot}10^{-4}$	0	-	0.5
2	Cu^{N}-Co^{N}	$6{\cdot}10^{-3}$	0	198.3	1.3
3	Cu^{N}-Co^{N}	$6{\cdot}10^{-2}$	0	197.5	2.4
4	Cu^{N}-Co^{N}	0	$6{\cdot}10^{-4}$	198.1	0.4
5	Cu^{N}-$Co^{N}_{[0.5M]}$	0	0	198.1	2.3

Table S5. Adsorption energies (eV) of FUR and FAL on Co(111) and Co(0001) in parallel **a** and perpendicular **b** modes at different Cl coverages.

Adsorption energies / eV					
θ(Cl)	**Species**	**Mode**	**Mode a**	**Mode b**	**(a – b)**
0.00	FUR	Co(111)	-1.93	-0.84	-1.09
	FUR	Co(0001)	-2.04	-0.85	-1.19
	FAL	Co(111)	-1.66	-0.82	-0.84
	FAL	Co(0001)	-1.74	-0.83	-0.91
0.06	FUR	Co(111)	-1.95	-0.88	-1.07
	FUR	Co(0001)	-2.08	-0.91	-1.17
	FAL	Co(111)	-1.71	-0.86	-0.85
	FAL	Co(0001)	-1.87	-0.89	-0.98
0.25	FUR	Co(111)	-1.07	-0.91	-0.16
	FUR	Co(0001)	-1.14	-0.91	-0.23
	FAL	Co(111)	-1.17	-0.88	-0.29
	FAL	Co(0001)	-1.28	-0.89	-0.39
0.31	FUR	Co(111)	-0.56	-1.04	+0.48
	FUR	Co(0001)	-0.41	-1.18	+0.77
	FAL	Co(111)	-0.44	-1.07	+0.63
	FAL	Co(0001)	-0.57	-1.12	+0.55